Observation of Buried Interfaces with Low Energy Electron Microscopy

R. M. Tromp, A. W. Denier van der Gon, F. K. LeGoues, and M. C. Reuter
IBM Research Division, T. J. Watson Research Center, P.O. Box 218, Yorktown Heights, New York 10598
(Received 18 August 1993)

In this Letter we show that a coherent low energy electron beam (<100 eV) can be used to obtain real space images of structures and defects buried deep below the surface of the sample. The elastic strain fields of such buried structures, extending to the free surface, are found to give rise to localized phase shifts in the reflected electron waves, resulting in excellent image contrast under slight objective lens defocus conditions. We can now image the formation and evolution of buried interfaces and defects *in situ*, and in real time. Because of the very low electron energies used, this imaging method is nondestructive.

PACS numbers: 61.16.–d, 61.72.Ff, 68.35.Ja

The formation, structure, and evolution of buried interfaces is of crucial importance in a wide range of materials systems and applications. Since interfaces are necessarily embedded in a solid they are difficult to study, requiring probes with large penetration depth. Nonspatially resolving techniques include Rutherford backscattering spectroscopy (RBS) [1], medium energy ion scattering (MEIS) [2], x-ray scattering [3], or electron transport measurements [4] across the interface. To obtain spatial resolution, destruction of the sample is often unavoidable. In this category the most widely used technique is transmission electron microscopy (TEM) [5]. Before TEM observation a sample is thinned down in plan-view or cross-section geometry. When sufficiently thin, the sample is transparent at the high electron energies used (100–400 keV), and the buried interface may be observed with high spatial resolution. Imaging of dislocations and extended defects in the TEM relies on the presence of elastic strain fields around such defects. These give rise to a local change in diffraction conditions, which can result in contrast in the image. Here we demonstrate that these same strain fields can be imaged with an electron beam of 4–5 orders of magnitude lower energy, on standard samples, and *in situ*.

Recent STM experiments have shown that strain fields associated with interfacial defects may extend all the way up to the surface of an epitaxial film [6,7]. If the dislocations are far apart the *amplitude* of the surface displacements remains constant, but the *width* of the displacement field increases linearly with thickness. If the dislocations are close together, their strain fields will overlap and the displacements at the surface damp out quickly with increasing film thickness. Low energy electron microscopy (LEEM) uses reflected electrons (typically 0–100 eV) to form images of the surface. Because of the low electron energy the technique is very surface sensitive. Below ~ 20 eV the electron penetration depth increases sharply, and the imaging process integrates over a sample thickness that may exceed 100 Å. This results in excellent sensitivity for small displacement fields extending across the thickness of a thin film.

We have used LEEM to study the growth of epitaxial Ag(111) islands on a Si(111) substrate. In addition to atomic steps on top of the Ag islands we observe atomic steps at the Si/Ag interface, interface dislocations, and stacking faults in the Ag islands. Interfacial structure was observed below islands as thick as 700 Å, as measured with atomic force microscopy (AFM). Dislocation structures observed with LEEM were also studied with plan-view TEM, confirming their nature and their location at the Si/Ag interface. With LEEM, observations can be made in real time during thin film growth, while strain relaxation (due to lattice mismatch, differential thermal expansion, composition grading, etc.) proceeds on standard samples that do not need to be thinned, and over a wide range of temperatures. Because of the parallel nature of the imaging process, a wide field of view is accessible at videorate.

LEEM was developed in recent years by Bauer and Telieps [8]. In our laboratory we have designed and built a LEEM instrument to study surface and interface dynamics, with a lateral resolution of ~ 150 Å. Single height atomic steps can be observed by slightly defocusing the microscope, taking advantage of the phase difference between electron waves reflected from the top and the bottom of the atomic steps (so-called phase contrast). In this study, the incident electron beam was aligned along the surface normal, and the (0,0) beam (exiting along the surface normal) was used for image formation (bright field imaging condition). A full description of this microscope [9] as well as recent results [10] have been published elsewhere.

Many studies have been performed on the formation of the Si(111)/Ag interface [11]. Below 1 monolayer coverage Ag may give rise to (3×1) and $(\sqrt{3}\times\sqrt{3})R30°$ reconstructions, if deposited at elevated temperature. At higher coverage Ag is found to form epitaxial islands. The ratio of Si to Ag lattice constants is almost exactly equal to 4:3 (within 0.3% at room temperature), giving rise to excellent epitaxy. Four Ag lattice planes fit onto three Si lattice planes, with an unreconstructed Ag/Si interface [12]. [Since the linear thermal expansion coefficient of Ag is 4 times larger than that of Si (19×10^{-6} vs $4.7\times10^{-6}\,°C^{-1}$), this mismatch increases with temperature.] In this work we deposited Ag at a rate of ~ 1 monolayer per minute, at a sample tempera-

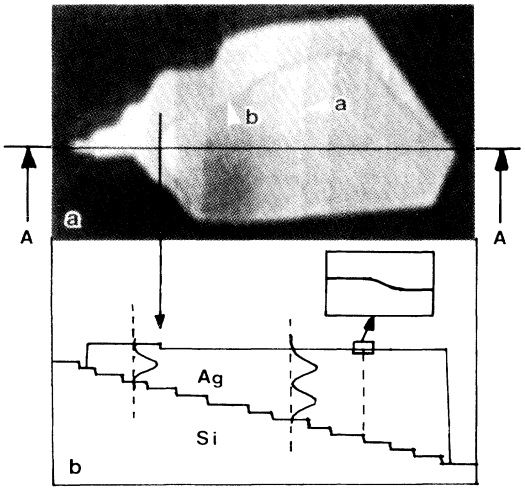

FIG. 1. (a) LEEM image of epitaxial Ag island on Si(111). Arrow *a*: atomic step at Si/Ag interface. Arrow *b*: atomic step on top of the Ag island. (b) Schematic cross section of (a) along line *A-A*. The vertical scale is greatly exaggerated. With increasing Ag thickness, more electron wavelengths can be fitted between surface and interface, as shown schematically. The inset shows how misfit strain at the interface extends up to the surface of the Ag island, where it can give rise to phase contrast.

ture of ~200 °C. Under these conditions the epitaxial islands can grow to considerable lateral extension (up to ~20 μm), ideal for studies of the interface. Figure 1(a) shows a LEEM image of a growing island. The Ag island appears bright, the surrounding Si surface is dark. The image was taken at slight out-of-focus condition, to reveal surface and interface steps by phase contrast. Several features can be observed in this image, as schematically highlighted in Fig. 1(b). First, strong contrast is observed due to atomic steps on the Si surface at the Si/Ag interface (vertical bright/dark lines, see arrow *a*). While not visible in the image shown here, these lines continue on the Si surface surrounding the island, showing directly that these steps are associated with the Si substrate. In addition a single height atomic step is observed on top of the island (arrow *b*). Under the dynamic growth conditions under which this image was taken, this step was seen to sweep across the island, while the interface steps remained stationary. Apart from this single step, the surface of the island is atomically smooth. Additionally, the brightness of the island image changes from terrace to terrace in a cyclical fashion. The periodicity and the phase of this cyclical contrast variation depends on the wavelength of the incident electrons. With increasing wavelength (lower electron energy) the contrast bands shift towards the thicker regions of the island, while the spacing between bright bands increases. A similar effect can also be seen in Fig. 1(a), where the contrast bands jump to the left upon crossing the single height atomic step on top of the Ag crystal in the step-up direction (arrow *b*). These intensity variations arise from interference between electron waves reflected from the surface of the thin crystal and from the Si/Ag interface. Such interference effects have been observed with LEEM previously by Bauer [13] and were reported even earlier by Park *et al.* [14]. In Fig. 1(b) we show schematically how the number of electron wavelengths matching the thickness of the film increases with film thickness, explaining the cyclical nature of the contrast variations. We observe these quantum well states only in very thin crystals, when the penetration depth of the electrons exceeds the film thickness. Figure 2 shows another, larger island as observed with AFM [Fig. 2(a)] and with LEEM [Fig. 2(b)]. The AFM image was obtained in air, after removal of the sample from the UHV LEEM system. In Fig. 2(b) we see interface atomic steps as in Fig. 1 (arrows *a*), as well as a high density of surface steps (arrows *b*), indicating large variations in thickness across the island. In addition, straight lines traverse the islands in some places, stopping or turning abruptly (arrows *c*). These latter features suddenly occurred after growth was stopped and the sample was cooling down to room temperature. They appear from one video frame to the next, i.e., within 30

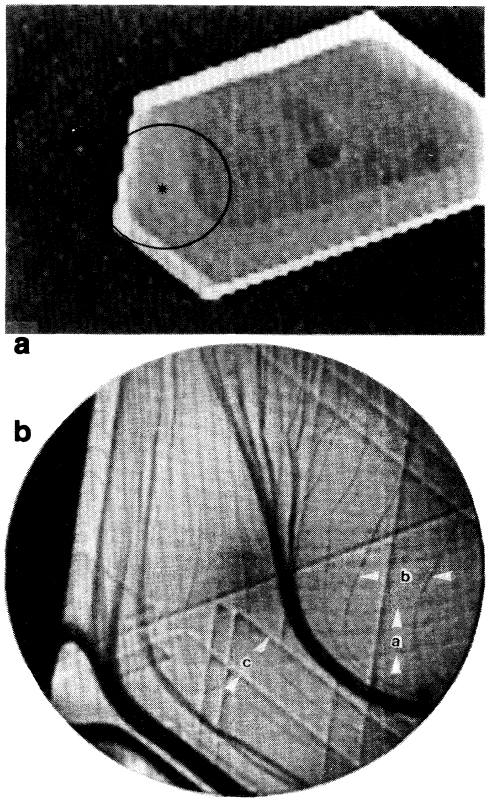

FIG. 2. (a) AFM image of epitaxial Ag island. A LEEM image of the circled region is shown in (b). Field of view in (b) is 4 μm. Arrows *a*: interface steps. Arrows *b*: surface steps. Arrows *c*: stacking faults.

ms, indicating a growth speed of at least 0.2–0.5 mm/s. These features are identified as stacking faults on Ag {111} planes intersecting the (111) surface, extending from the interface to the surface. They form due to the difference in thermal expansion between Ag and Si. Reheating the sample to the growth temperature removes the stacking faults in many cases. In some cases stacking faults occur during growth, probably due to slight deviation from exact 3:4 lattice match. Figure 2(a) shows an AFM image of the same island. The area marked by the asterisk in Fig. 2(a) is 700 Å thick, not thick enough to suppress observation of the Si/Ag interface as seen in Fig. 2(b).

Figure 3 shows yet another Ag island, immediately after growth was stopped [3(a)], and after the sample was allowed to cool to room temperature for 2 h [3(b)]. In Fig. 3(b) a number of lines are observed at the Ag/Si interface, which we identify as interface misfit dislocations (arrows *a*). Also some stacking faults are seen (arrows *b*). Plan-view TEM images of similar islands show very similar features. In Fig. 3(c) the TEM image was obtained in the ⟨220⟩ two-beam condition, which highlights the dislocations at the Si/Ag interface. To obtain more information on the interfacial regions *between* dislocations the same area was also imaged in a 1/3⟨422⟩ two-beam condition. While the 1/3⟨422⟩ reflections are symmetry forbidden in the bulk, they are allowed at surfaces and interfaces due to the reduced symmetry. The resulting image [Fig. 3(d)] shows three distinct contrast

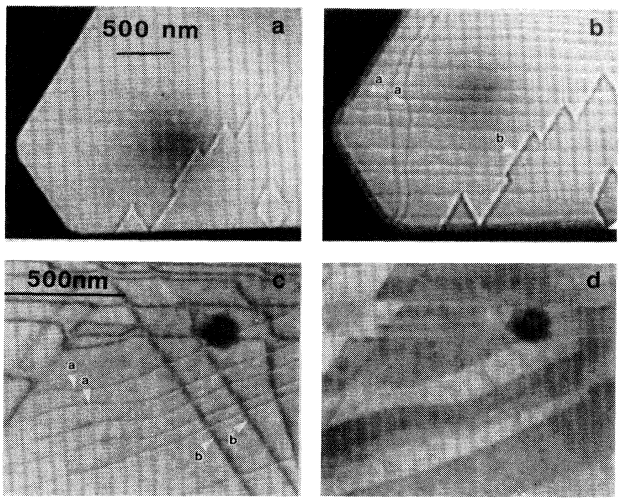

FIG. 3. (a) LEEM image of Ag island directly after growth at 200 °C. (b) Same region after cooldown to room temperature. (c) Plan-view TEM image in ⟨220⟩ two-beam condition, highlighting interface dislocations at the Si/Ag interface. (d) Plan-view TEM image in 1/3⟨422⟩ two-beam condition, showing three distinct grey levels between dislocation lines. This indicates that the dislocations have partial dislocation character [same region as (c)]. Arrows *a*: interface dislocations [not present in image (a)]. Arrows *b*: stacking faults.

levels in the interfacial areas between dislocations. This shows that there are three distinct stacking sequences at the Si/Ag interface, and that the interface stacking sequence changes upon crossing a dislocation line. Thus, Fig. 3(d) provides direct evidence that the dislocations have partial dislocation character. Unfortunately a more detailed analysis of these dislocations is hampered by the fact that the diffraction pattern includes reflections from both Si and Ag, with a difference in lattice constants of 25%. This makes it impossible to set up *exact* diffraction conditions needed to determine the Burgers vector of the dislocations, because they can be exact only relative to one of the two lattices (Ag or Si) at a time. Nonetheless, it is clear that these are partial dislocations, injected at the Si/Ag interface from the edges of the epitaxial islands. These dislocations relieve the residual misfit strain, relative to the almost exact 3:4 lattice match between Si and Ag. With LEEM the formation of this dislocation network can be observed in real time, during cooling or heating from the growth temperature.

In LEEM the interface steps and dislocations, as well as the surface steps can be seen in both underfocus and overfocus conditions, but not when the island is exactly in focus. [For instance, Fig. 3(a) was taken in overfocus, Fig. 3(b) in underfocus.] This indicates that these features are observed due to phase contrast. In the following we discuss the contrast mechanism in more detail. The interface steps consist of steps in the original starting Si surface, accompanied by steps in the Ag crystal which are subjected to the full 25% lattice mismatch. This gives rise to a large and extended strain field. Recent STM studies show that such strain fields extend to the surface of the film. For the Si/Ag interface atomic steps this is shown schematically in the inset of Fig. 1(b). If the dislocations are widely separated the amplitude of the strain field does not diminish with thickness, but the width increases linearly with thickness. Thus, as long as the range of displacements *at the surface of the Ag islands* is large enough within the lateral coherence length of the electron beam (several 100 Å), good phase contrast is obtained. The fact that the contrast arises from an extended strain field also explains why the contrast is strong. Instead of interference between phase-shifted waves reflected from a single atomic layer (as is the case at the surface step), we observed interference between phase-shifted waves reflected over the penetration depth of the electrons. Interface steps, interface dislocations, and stacking faults are all accompanied by such extended strain fields, and are also observed in phase contrast.

The results shown in Fig. 1 show that if the film is sufficiently thin electrons reflected from the *interface* contribute to the image as well, but give rise to a fundamentally different (quantum-size) contrast, which does not depend on defocus. When the film thickness increases beyond the penetration depth of the electrons (such as in Figs. 2 and 3) these quantum well states are no longer observed. Thus, even when the electrons do not reach the

interface, interface features can still be seen, giving additional evidence that strain fields extending to the surface of the thin films enable the observation of interface steps and defects.

Deeply buried interfaces can be observed with LEEM. We have determined that defect related strain fields extending to the surface of the growing film give rise to phase contrast, enabling the observation of interfacial features. Such strain fields were observed with STM in the $Si/CoSi_2$ and Si(111)/Ge systems. The Si(111)/Ge system (stabilized with a Sb surfactant monolayer [15]) was recently studied in detail with spot-profile-analysis low energy electron diffraction (SPA-LEED) [16]. This technique uses an electron beam very similar to that employed in LEEM. When the Ge film exceeds the critical thickness for dislocation injection at the Si/Ge interface, a regular network of partial dislocations is formed to relieve the 4.3% misfit strain in the Ge film. The strain fields associated with this network were observed directly with STM in Ref. [6]. In the SPA-LEED experiments the ordered strain-field network at the surface of the Ge film gives rise to splitting of the diffracted beams. The diffracted intensities can be analyzed quantitatively to reconstruct the surface strain fields, yielding a vertical amplitude of the surface strain field of 0.5 Å at 50 Å film thickness. In SPA-LEED spot splitting is observed when the dislocation network is ordered. Disordered networks give rise to spot broadening, and widely separated dislocations [as in Fig. 3(b)] would not be observed. Interestingly, the strain fields that are detected in the SPA-LEED experiment can be directly imaged in LEEM, independent of order and also at very low density.

Wherever there are extended defects (interface steps, dislocations, stacking faults) they are accompanied by long range strain fields. These strain fields are accessible to imaging by LEEM, as they are to imaging by TEM. An important advantage of LEEM is that no special sample preparation is required, and *in situ* observation during growth and over a large field of view is straightforward. An important advantage of TEM is that the dislocations may be imaged in a number of different diffraction conditions, in general allowing determination of the Burgers vector. Using weak-beam imaging techniques the TEM also allows for higher resolution imaging than LEEM. Thus, LEEM and TEM are powerful complementary techniques for studying interface formation and structure.

We are presently investigating the injection of misfit dislocations in the $Si(111)/CaF_2$ system, where—again—strong phase contrast is observed for interface defects. Although CaF_2 is extremely radiation sensitive, we find that it can be imaged during growth at 700 °C without problems, and without beam-induced changes. We attribute this to the very gentle interaction of the low energy electron beam with the sample. LEEM promises to be particularly valuable for *in situ* studies of epitaxial interface formation and defect evolution in a number of scientifically and technologically interesting materials systems.

We gratefully acknowledge the assistance of Yves Martin in obtaining the AFM results, and we thank John Ott for his patience and expertise in TEM sample preparation. One of the authors (A.W.D.v.d.G.) was partially supported by the Stichting voor de Technische Wetenschappen (Dutch Technology Foundation).

[1] W. K. Chu, J. W. Mayer, and M. A. Nicolet, *Backscattering Spectrometry* (Academic, New York, 1978).
[2] J. F. van der Veen, Surf. Sci. Rep. **5**, Nos. 5/6 (1985).
[3] A. Bourret, P. Fuoss, G. Feuillet, S. Tatarenko, Phys. Rev. Lett. **70**, 311 (1993), and references therein.
[4] See, for instance, R. T. Tung, Phys. Rev. Lett. **50**, 461 (1984).
[5] See, for instance, *High Resolution Microscopy of Materials*, edited by W. Krakow, F. A. Ponce, and D. J. Smith, MRS Symposia Proceedings No. 139 (Materials Research Society, Pittsburgh, 1989).
[6] G. Meyer, B. Voigtländer, and N. Amer. Surf. Sci. **274**, L541 (1992).
[7] R. Stalder, H. Sirringhaus, N. Onda, and H. von Känel, Ultramicroscopy **42-44**, 781 (1992).
[8] E. Bauer, Ultramicroscopy **17**, 51 (1985); W. Telieps and E. Bauer, Ultramicroscopy **17**, 57 (1985).
[9] R. M. Tromp and M. C. Reuter, Ultramicroscopy **36**, 99 (1991); Mater. Res. Soc. Symp. Proc. **237**, 349 (1992).
[10] R. M. Tromp and M. C. Reuter, Phys. Rev. Lett. **68**, 820 (1992).
[11] See A. W. Denier van der Gon and R. M. Tromp, Phys. Rev. Lett. **69**, 3519 (1992), and references therein.
[12] F. K. LeGoues and P. S. Ho, Philos. Mag. A **53**, 833 (1986).
[13] M. Mundschau, E. Bauer, and W. Swiech, J. Appl. Phys. **65**, 581 (1989), and references therein.
[14] R. L. Park, B. T. Jonker, H. Iwasaki, and Q.-G. Zhu, Appl. Surf. Sci. **22/23**, 1 (1985).
[15] M. Horn-von Hoegen, F. K. LeGoues, M. W. Copel, M C. Reuter, and R. M. Tromp, Phys. Rev. Lett. **67**, 1130 (1991).
[16] M. Horn-von Hoegen, M. Pook, A. Al Falou, B. H. Müller, and M. Henzler, Surf. Sci. **284**, 53 (1993).

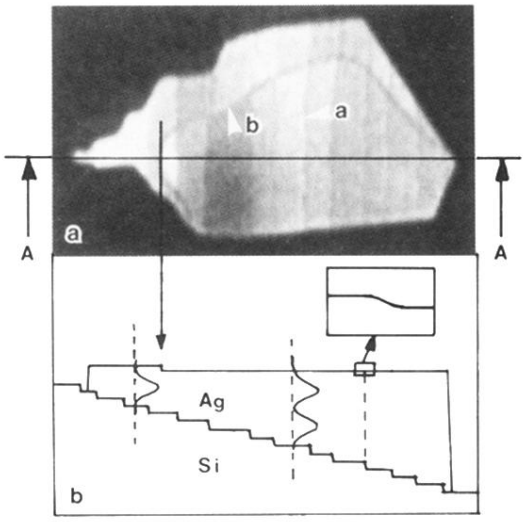

FIG. 1. (a) LEEM image of epitaxial Ag island on Si(111). Arrow *a*: atomic step at Si/Ag interface. Arrow *b*: atomic step on top of the Ag island. (b) Schematic cross section of (a) along line *A*-*A*. The vertical scale is greatly exaggerated. With increasing Ag thickness, more electron wavelengths can be fitted between surface and interface, as shown schematically. The inset shows how misfit strain at the interface extends up to the surface of the Ag island, where it can give rise to phase contrast.

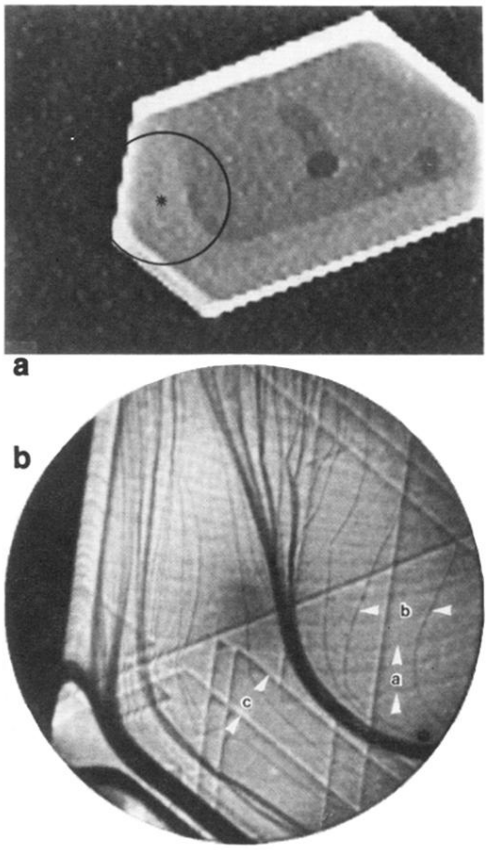

FIG. 2. (a) AFM image of epitaxial Ag island. A LEEM image of the circled region is shown in (b). Field of view in (b) is 4 μm. Arrows *a*: interface steps. Arrows *b*: surface steps. Arrows *c*: stacking faults.

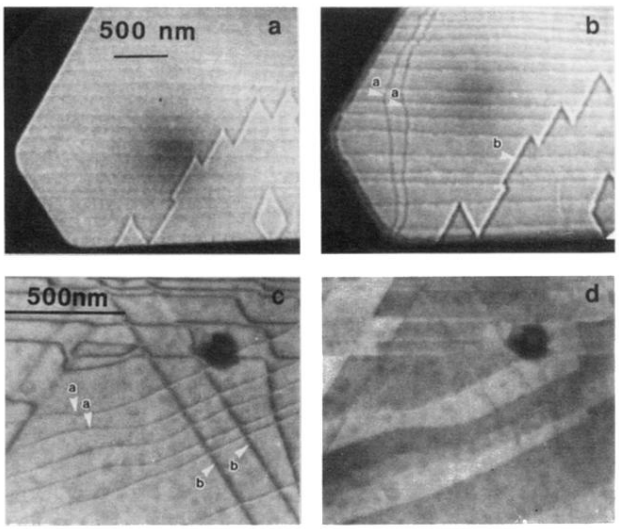

FIG. 3. (a) LEEM image of Ag island directly after growth at 200 °C. (b) Same region after cooldown to room temperature. (c) Plan-view TEM image in ⟨220⟩ two-beam condition, highlighting interface dislocations at the Si/Ag interface. (d) Plan-view TEM image in 1/3⟨422⟩ two-beam condition, showing three distinct grey levels between dislocation lines. This indicates that the dislocations have partial dislocation character [same region as (c)]. · Arrows *a*: interface dislocations [not present in image (a)]. Arrows *b*: stacking faults.